Geophysical Research Letters

RESEARCH LETTER
10.1029/2018GL080890

Key Points:
- Recent and prehistoric flood deposits are recorded in Chesapeake Bay sediments
- Flood frequency is higher during negative phases of the North Atlantic Oscillation
- Negative NAO conditions may increase hurricane landfalls along the U.S. East Coast

Supporting Information:
- Supporting Information S1
- Data Set S1

Correspondence to:
M. Toomey,
mtoomey@usgs.gov

Citation:
Toomey, M., Cantwell, M., Colman, S., Cronin, T., Donnelly, J., Giosan, L., et al. (2019). The mighty Susquehanna—Extreme floods in eastern North America during the past two millennia. *Geophysical Research Letters*, *46*, 3398–3407. https://doi.org/10.1029/2018GL080890

Received 12 OCT 2018
Accepted 15 FEB 2019
Accepted article online 19 FEB 2019
Published online 20 MAR 2019

The Mighty Susquehanna—Extreme Floods in Eastern North America During the Past Two Millennia

Michael Toomey[1], Meagan Cantwell[2], Steven Colman[3], Thomas Cronin[1], Jeffrey Donnelly[3], Liviu Giosan[3], Clifford Heil[4], Robert Korty[5], Marci Marot[6], and Debra Willard[1]

[1]Florence Bascom Geoscience Center, U.S. Geological Survey, Reston, VA, USA, [2]Department of Geology, College of William and Mary, Williamsburg, VA, USA, [3]Department of Geology and Geophysics, Woods Hole Oceanographic Institution, Woods Hole, MA, USA, [4]Graduate School of Oceanography, University of Rhode Island, Narragansett, RI, USA, [5]Department of Atmospheric Sciences, Texas A&M University, College Station, TX, USA, [6]St. Petersburg Coastal and Marine Science Center, United States Geological Survey, St. Petersburg, FL, USA

Abstract The hazards posed by infrequent major floods to communities along the Susquehanna River and the ecological health of Chesapeake Bay remain largely unconstrained due to the short length of streamgage records. Here we develop a history of high-flow events on the Susquehanna River during the late Holocene from flood deposits contained in MD99-2209, a sediment core recovered in 26 m of water from Chesapeake Bay near Annapolis, Maryland, United States. We identify coarse-grained deposits left by Hurricane Agnes (1972) and the Great Flood of 1936, as well as during three intervals that predate instrumental flood records (~1800–1500, 1300–1100, and 400–0 CE). Comparison to sedimentary proxy data (pollen and ostracode Mg/Ca ratios) from the same core site indicates that prehistoric flooding on the Susquehanna often accompanied cooler-than-usual winter/spring temperatures near Chesapeake Bay—typical of negative phases of the North Atlantic Oscillation and conditions thought to foster hurricane landfalls along the East Coast.

Plain Language Summary Despite the vulnerability of many mid-Atlantic cities to flooding, including Washington D.C., few long-term records exist to assess the risks posed by extreme, infrequent, storm events. Here we document recent and prehistoric floods on the Susquehanna River, which has the largest watershed on the U.S. Eastern Seaboard, using sediment cores collected from Chesapeake Bay. Our analysis finds that much of the Susquehanna's observed centennial-millennial scale flood variability may be driven by the frequency of hurricane landfalls along the U.S. East Coast.

1. Introduction

On 21 and 22 June 1972, more than 25 cm (10 in.) of rain fell across areas of southeastern Pennsylvania as Hurricane Agnes came ashore (Bailey et al., 1975; Figure 1). Two days later, the Susquehanna River near Harrisburg, Pennsylvania, swelled to a record ~5 m (16 ft) above flood stage (Bailey et al., 1975). Floodwaters deposited an estimated ~30 × 10^6 m^3 of sediment downstream in the Chesapeake Bay (Zabawa & Schubel, 1974), smothering aquatic vegetation and degrading fisheries (Andersen et al., 1973). Damage from Agnes, mostly in Pennsylvania, exceeded $3 billion (approximately $19 billion in 2018 dollars) making it the costliest hurricane in U.S. history at the time (Bailey et al., 1975). Since 1972, three other cyclones—Eloise (1975), Ivan (2004), and Lee (2011; Figure 1d)—have pushed the Susquehanna above major flood stage (USGS, 2018) with similar, though less severe, downstream effects.

Tropical cyclones, or extratropical cyclones interacting with a front, are the primary and secondary drivers of extreme rainfall along the U.S. East Coast (Kunkel et al., 2012). Daily U.S. rain-gage data from 1936 to 1996 indicate tropical cyclone rainfall exceeding 10 cm (~4 in.) occurs at timespans of less than 20 years along much of the Eastern Seaboard and Gulf Coast (Hart & Evans, 2001). Villarini et al. (2014) found peak discharge during tropical cyclone passage often surpassed the 10-year flood peak at U.S. Geological Survey (USGS) gage stations within 500 km of each storm's track. Tropical cyclone flooding on East Coast rivers occurred more frequently (~70%) when the May–June North Atlantic Oscillation (NAO) index, most often described by the normalized monthly sea level pressure difference between

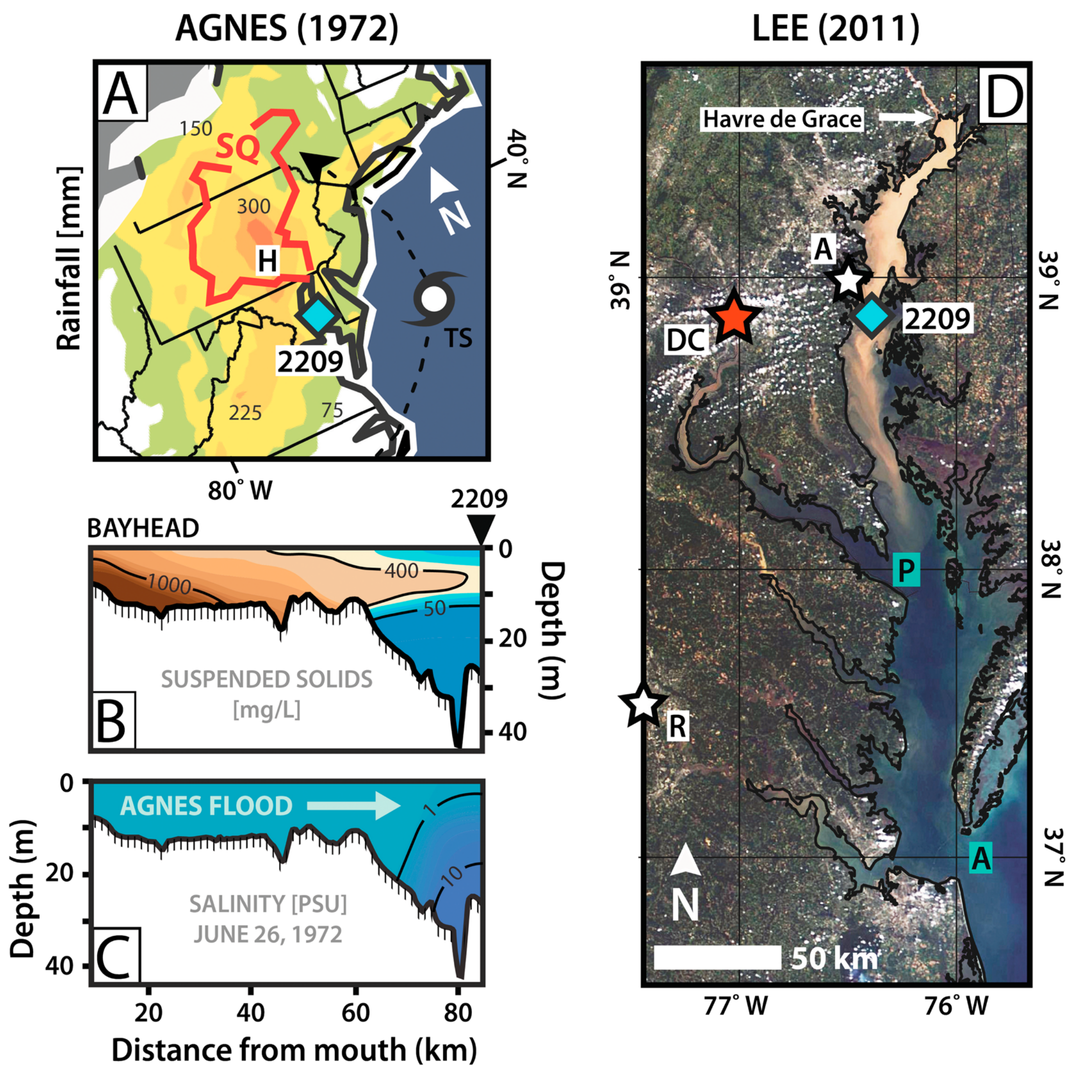

Figure 1. Geologic setting. (a) Eastern United States rainfall during hurricane Agnes (14–25 June 1972; PSD-NOAA: U.S. Unified Precipitation data [https://www.esrl.noaa.gov/psd/]). Dashed line follows storm track. Susquehanna watershed outlined in red. "H" gives location of Harrisburg, Pennsylvania. (b) Suspended solid concentration and (c) salinity profiles along the main stem of Chesapeake Bay on 26 June 1972 following hurricane Agnes—both panels adapted from Schubel (1974) and reprinted with permission. Distance (*x* axis) is expressed in kilometers from Havre de Grace, Maryland, the mouth of the Susquehanna River. Location of RD98/MD99-2209 approximate. (d) Sediment plume following Tropical Storm Lee (2011). Satellite (NASA [https://earthobservatory.nasa.gov/images/52169/sediment-clouds-the-chesapeake-bay]) image from 13 September 2011. Mouth of the Potomac River and its outlet into the open North Atlantic given by aqua highlighted "P" and "A," respectively. Stars: Washington (DC), Annapolis (A), and Richmond (R).

Portugal and Iceland (e.g., Jones et al., 1997), was negative (Villarini et al., 2014). Tropical systems that have transitioned, or are undergoing transition, into extratropical storms—like Hurricane Agnes (1972)—have brought some of the heaviest rainfall to the Northeastern United States, a process also weakly, negatively, correlated, with the NAO (Hart & Evans, 2001).

Storm deposits have been used to link prehistoric North Atlantic hurricane activity to the NAO (Denommee et al., 2014, etc.) as well as other forcings such as the El Niño-Southern Oscillation, changes in local sea surface temperature (SST), and the Atlantic Meridional Overturning Circulation (e.g., Brandon et al., 2013; Donnelly & Woodruff, 2007; Toomey et al., 2017). However, the population of intense North Atlantic hurricanes that cause coastal flooding may not be the same as the storms that produce intense rainfall and high river flows. Only a handful of geologic proxy reconstructions of high flows currently exist for Eastern North American river systems (Munoz et al., 2018; Oliva et al., 2016, etc.); but estuaries, which capture terrestrial sediment shed during floods, likely record these past events. For instance, shallow sediment cores recovered from Northern Chesapeake Bay after Hurricane Agnes (1972; Zabawa & Schubel, 1974) and Tropical Storm Lee (2011; Palinkas et al., 2014) contained deposits centimeters thick.

Here we identify sedimentary deposits left by Hurricane Agnes, as well as other large floods in a set of piston cores collected near Annapolis, Maryland, in order to address two main questions:

1. Do Chesapeake Bay sediments record extreme, prehistoric floods of the Susquehanna River?
2. Is there a relationship between the frequency of high flows and the NAO and/or North Atlantic SSTs?

2. Geologic Context

2.1. Study Site

The Susquehanna watershed (71,250 km^2) encompasses a large portion of the northern Appalachian Mountains where it extends across parts of three U.S. states (Maryland, New York, and Pennsylvania) and supplies ~1,100 m^3/s of fresh water, on average, to the Chesapeake Bay estuary (Schubel & Pritchard, 1986). In most years, the highest monthly discharges occur in March or April during the spring freshet, often exceeding 10,000 m^3/s. Annually, the Susquehanna delivers ~2×10^6 t of sediment to Chesapeake Bay (Gross et al., 1978; Officer et al., 1984). Much of this material is, however, trapped within 60–80 km of the river's mouth (Eaton et al., 1980); little is transported south of the Potomac River (Figure 1d) or to the open North Atlantic, ~180 and 300 km from the bay head, respectively. Thick deposits of estuarine sediments (Colman et al., 1992), often laminated (Ryan, 1953), have accumulated in Northern Chesapeake Bay since sea level inundation ~8 Kyr BP (Cronin et al., 2007), especially in the deep (>30 m below sea level) main channel that runs along the Bay's eastern margin. These deposits were targeted by Calypso core MD99-2209 (38° 53.18′ N, 76° 23.68′ W) and collected during June 1999 by the R/V *Marion Dufresne* (IMAGES V Cruise) in 26 m of water (Halka et al., 2001) near Annapolis, Maryland, ~85 km from the Susquehanna's Mouth. The core was subsequently split into 1.5-m-long sections and archived at the USGS in Woods Hole, Massachusetts, and University of Rhode Island. The RD98 series kasten (K1,2) and piston (P1,2) cores, recovered at the same approximate location in November 1998 (Baucom et al., 2001) and MD03-2661 (e.g., Cronin et al., 2010) collected ~300 m east of our site in 2003, are also discussed in the text below.

2.2. MD99-2209 Sedimentology and Stratigraphy

A mixture of siliciclastic minerals, salts, organic matter, and marine fauna (ostracodes, benthic foraminifera, diatoms, and mollusks) composes the sediment of MD99-2209. X-ray diffraction analysis of a sample from 285–290 cm identified quartz, feldspar, and clay (illite) as the dominant mineral constituents, consistent with previous analysis of Chesapeake Bay sediments (Powers, 1954; Ryan, 1953). Gypsum is also present in small quantities, similar to cores collected from the deep main channel collected near the mouth of the Patuxent River reported by Cann and Cronin (2004). Within the coarse-silt fraction (32–63 μm), ~90 and 8% of the mineral material is quartz and feldspar, respectively. Organic content is generally low (1–3%) with $\delta^{13}C$ ranging from −22 to −24 (‰ PDB) in RD98 (Baucom et al., 2001). High C/N ratios (up to 15), compared to a background of about 8, occur between ~50 and 175 cm (RD98; Baucom et al., 2001) mirroring Pennsylvania anthracite production (Milici & Campbell, 1997). Two very large (~1 cm^3) charcoal pieces were found at 179 and 191 cm in MD99-2209.

Based on shipboard descriptions (Baucom et al., 2001) and our more recent observations of the core, the late Holocene section of MD99-2209 can be divided into three main stratigraphic units (Figure 2, right). (1) Sediment from the surface down to a sharp contact at 280 cm is laminated silt and clay with lower density than the sediments below. (2) Mostly uniform, more massive, clayey silts are found from ~280–730 cm depth. (3) Sand increases beginning at 730 cm, particularly through a time-condensed section from 810–830 cm that separates the late and mid-Holocene. Its origin, attributed to a number of possible processes by Halka et al. (2001; e.g., winnowing by tidal currents and changes in site geometry) is beyond the scope of this manuscript, which will focus solely on the late Holocene section (above 7.5-m core depth).

3. Methods

Standard wet sieving techniques were used to separate the >32-μm fraction from bulk sediment sampled downcore at 1-cm intervals. Each sample was then dry-sieved at >63 μm to isolate the silt size fraction from (1) relic fine/medium-grained sands (well-sorted) potentially transported from shallow water areas offshore

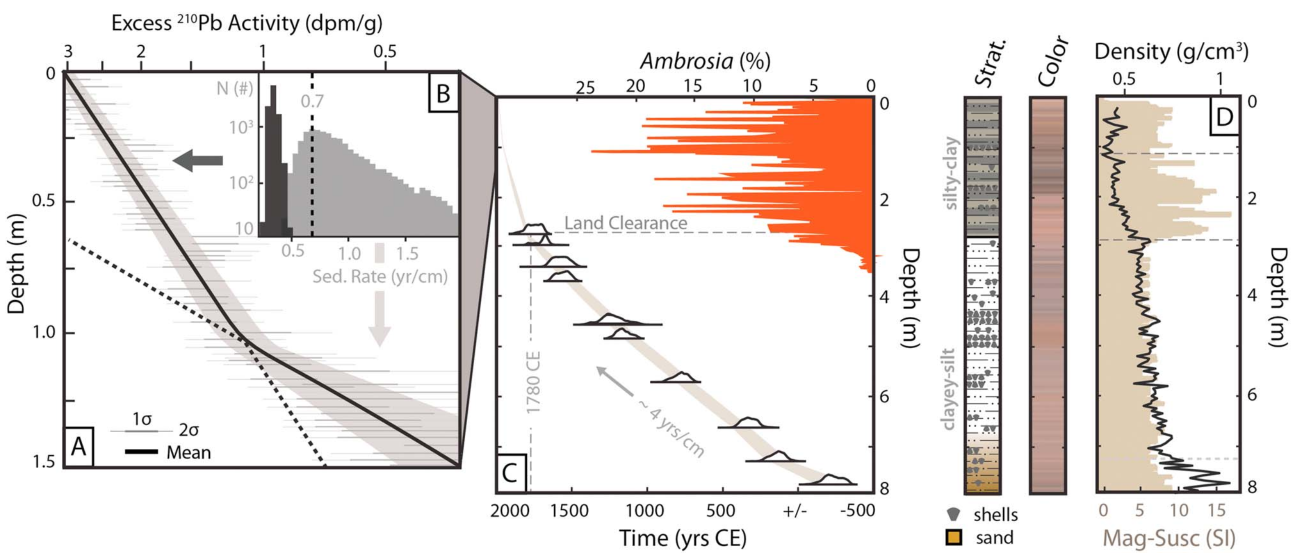

Figure 2. Age model and stratigraphy of MD99-2209. (a) Excess ^{210}Pb activity during historic deposition (magnification of ^{210}Pb chronology in (c)). Gray shading (black line) shows the one-sigma range (mean) of 10,000 modeled ^{210}Pb profiles used to calculate the (b) dark and light gray histograms (graphical sedimentation rate estimates) for the upper and lower slopes, respectively. (c) OxCal v4.3 (Ramsey, 2008) age model incorporating ^{210}Pb, ^{14}C, and land clearance (*Ambrosia*) horizons. Downcore stratigraphy (Baucom et al., 2000), sediment color of dry crushed samples, (d) density (dark gray line), and magnetic susceptibility (shaded brown; King & Heil, 2000).

Kent Island to the east (e.g. stations CB47/48 in Ryan, 1953) and (2) large gypsum crystals that may have formed in situ (e.g., Cann & Cronin, 2004). Grain-size variability was also estimated from relative zirconium and rubidium abundances (e.g., Davies et al., 2015) measured at ~1-mm intervals on u-channels using an Itrax X-ray florescence core scanner at the Woods Hole Oceanographic Institution. Rubidium, in general, adsorbs to the fine fraction, while zircon has been previously identified in the coarser sands of Chesapeake Bay sediments (Ryan, 1953). The log-normalized Zr/Rb ratio of a discrete, powdered, bulk sample taken from 285–290 cm in MD99-2209 was ~0.7 compared to 3.0 for the coarse-silt fraction alone. Downcore XRF log (Rb/Zr) measurements are complimentary to sieve-size data, allowing for better resolution of very thin (millimeter-scale) coarse-grained layers found in the finely laminated upper ~280 cm of MD99-2209.

Lead-210 (Figure 2a), radiocarbon, and fossil pollen (Figure 2c) were used to construct an age-depth model for MD99-2209. Ragweed (*Ambrosia*) pollen percentages were calculated at ~2-cm intervals from the top of MD99-2209 to a depth of 350 cm using standard palynological methods (e.g., Willard et al., 2003). Consistent with the existing literature, we suggest (1) an initial rise in ragweed pollen and magnetic susceptibility at ~280 cm corresponds with expansion of colonial agriculture around ~1780 CE in upper Chesapeake Bay (Brush, 1984) and mill dam construction in the Susquehanna watershed (Walter & Merritts, 2008), while (2) a later increase in sedimentation rate followed postwar urbanization (ca. 1960) of Chesapeake Bay, previously identified in Pocomoke Sound (Cronin, 2004). Prior to a dramatic decline of submerged aquatic vegetation in Northern Chesapeake Bay starting around 1960 (Orth & Moore, 1984), it is also possible more sediment was being captured nearshore and therefore not reaching our site in the deep main channel.

Total ^{210}Pb activity was measured in MD99-2209 using alpha spectroscopy and converted to age in three steps: (1) supported ^{210}Pb, estimated separately, from gamma counted ^{226}Ra activity (~1.7 ± 0.2 dpm/g), was subtracted from the total ^{210}Pb at each level. (2) A random draw was then taken from a normal distribution with the same mean and error of each of the resulting excess ^{210}Pb values. (3) A constant initial concentration model (Appleby & Oldfield, 1978, 1983) was used to convert these values to age with initial ^{210}Pb activity back-calculated from the ca. 1960 A.D. urbanization horizon. This approach accounts for potential loss of the sediment-water interface during piston coring and recovery. Repeated 10,000 times (Figure 2b) in Matlab (MathWorks®), we placed bounds on the age of each ^{210}Pb measurement and its uncertainty arising from gamma ray attenuation and machine counting errors.

Shell material from MD99-2209 and RD98 was radiocarbon dated (Figure 2c) at the National Ocean Sciences Mass Spectrometry facility in Woods Hole, Massachusetts, and previously reported by Colman et al. (2002). Each date was calibrated using the Marine13 reference curve (Reimer et al., 2013). We assumed no ΔR offset consistent with Cronin et al. (2005) and probability distributions for two ^{14}C age at 274 and 296 cm that overlap with the ~1780 CE colonial land clearance horizon at 280 cm. ^{14}C ages at 455 cm in MD99-2209 and 457 cm in RD98, both dating to 1,150 ^{14}C years (uncalibrated; Colman et al., 2002), indicate minimal offset between the two piston cores. For both, we calculated an age model using the Bayesian software program OxCal v4.3 (Ramsey, 2008) that incorporated the ^{210}Pb, ^{14}C, and pollen data described above.

The resulting chronology was used to interpolate grain size (percent coarse silt and XRF data) time series for MD99-2209 that could be compared to (1) discharge observations (Figures 3a and 3b) for the Susquehanna River at Harrisburg, Pennsylvania, (station: 0157050) available from the USGS National Water Information System (http://waterdata.usgs.gov/nwis), as well as the previously published (2) NAO reconstruction of Trouet et al. (2009; Figure 4b), (3) oxygen isotope data from Buckeye Creek Cave (West Virginia; Hardt et al., 2010; Figure 4b) and (4) percent pine pollen (Willard et al., 2003; Figure 4b) and (5) ostracode Mg/Ca data (Cronin et al., 2003, 2010) (Figure 4c) from RD98, MD99-2209, and MD03-2661.

4. Results and Discussion

Delivery of coarse silt to MD99-2209 is likely driven by salinity gradients and constrained by the geometry of upper Chesapeake Bay. In stratified estuaries, trapping of silt-sized material is enhanced near the landward edge of the incoming, saltier ocean water due to a decrease in turbulence (Geyer, 1993). During high Susquehanna flow conditions of the spring freshet, the Northern Chesapeake Bay salt wedge reaches as far North as Tolchester, MD (~45 km from the river's mouth; Schubel, 1974). Water sampling conducted after Hurricane Agnes (Figure 1c), however, showed the freshwater front displaced into much deeper, and typically saltier, waters found near Kent Island (Schubel, 1974; Schubel & Pritchard, 1986), nearly 80 km south of the river's mouth at Havre de Grace, Maryland. Suspended solids (Figure 1b) measurements suggest seaward advection of silt-laden flood-waters following Hurricane Agnes (1972) transported muddy sediments near our core site that are typically captured further up-estuary. A coarse-grained layer found near 60 cm in MD99-2209 dates to ~1970 (Figure 3c) and likely was deposited during this event. Relatively little coarse silt is available in shallow waters along the Eastern Shore near our site (Ryan, 1953) for transport by other mechanisms such as large storm surge or wave events (e.g. Hurricane Connie—1955).

Our grain-size time series, shown in Figure 3c, indicates that shallowly buried coarse layers in MD99-2209 likely reflect deposition following Hurricane Agnes (June 1972) as well as the Great Flood of March 1936—the two largest historic flood events on the Susquehanna River at Harrisburg, Pennsylvania. The largest grain-size peak in MD99-2209 deposited during the last hundred years occurs around ~1970, appears largely structureless in radiographs of RD98 (Baucom et al., 2001), and has low ^{210}Pb activity relative to adjacent depths, consistent with deposits in Chesapeake Bay previously attributed to Hurricane Agnes (Hirschberg & Schubel, 1979; Nie et al., 2001). A deeper coarse layer (2σ age $\approx$ 1933–1945) was likely deposited during the Great Flood of 1936. Both layers overlay intervals of minimal coarse-grained deposition likely corresponding to severe Pennsylvania droughts, during the early 1930s (Palmer Drought Severity Index < -6) and mid 1960s (Palmer Drought Severity Index < -4; NCDC, 2018) providing confidence in our age model.

Other major Susquehanna River floods recorded at this site may include Hurricane Eloise (1975) as well as three late spring (May/June) storms from 1889, 1894, and 1946, representing the ninth, third, fourth, and tenth largest historic events, respectively. Peak monthly rainfall at Harrisburg typically occurs in late spring (Koninklijk Nederlands Meteorologisch Instituut Earth Explorer; http://climexp.knmi.nl/), potentially, driving up soil moisture and creating favorable conditions for runoff during storms (e.g., Sturdevant-Rees et al., 2001). High rainfall preceding Hurricane Agnes is thought to have partially contributed to extreme water levels on the Conestoga River, a tributary of the lower Susquehanna River (Moss & Kochel, 1978). Historic accounts also link a May 1771 flood that exceeded hurricane Agnes, at least on the James River near Richmond, VA (~175 km SW), to an early season tropical cyclone (Blanton et al., 2009).

Altogether with MD99-2209′s (1) sheltered position relative to open-ocean teleseismic tsunamis, (2) low potential for locally triggered mass wasting, and (3) surveys showing substantial sediment deposition in

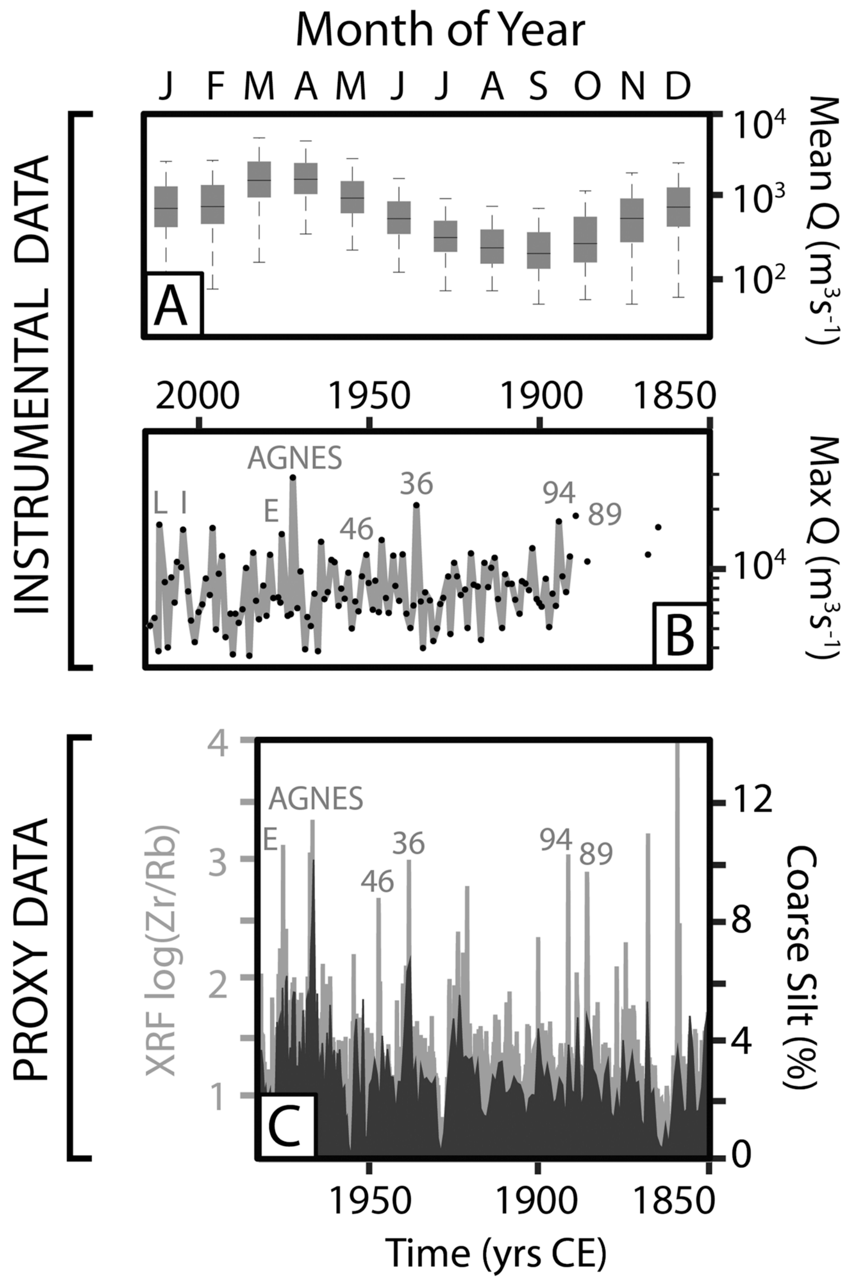

Figure 3. Comparison of instrumental streamgage data and proxy reconstruction of flood frequency. (a) Monthly mean Susquehanna River discharge (Q) at Harrisburg, Pennsylvania (USGS Station: 0157050; USGS, 2018), calculated from 1890–2017 CE observations. (b) USGS peak annual discharge at Harrisburg—intermittent data collected prior to 1890. (c) Coarse-grained deposition at MD99-2209 core-site. Black shading percent coarse-silt data, while gray shading gives XRF log (Zr/Rb) values. Large historic discharge peaks (b) and their inferred deposits (c) are numbered by year or labeled with a letter in the case of tropical storms Eloise "E," Ivan "I," and Lee "L."

Northern Chesapeake Bay following Hurricane Agnes (1972; Zabawa & Schubel, 1974) and Tropical Storm Lee (2011; Palinkas et al., 2014), we interpret downcore coarse-grained deposits in MD99-2209 (Figure 4d) from ~1800–1500, 1300–1100, and 400–0 CE as likely to be river-derived and often related to intense storm rainfall.

Delivery of large amounts of upland fluvial material to Northern Chesapeake Bay by recent and precolonial floods may have promoted low oxygen conditions. A north-south transect of cores extending from the RD98 core site to the Potomac River shows lower $\delta^{13}C$ values between ~1750–1400 and 1200–900 and

10.1029/2018GL080890

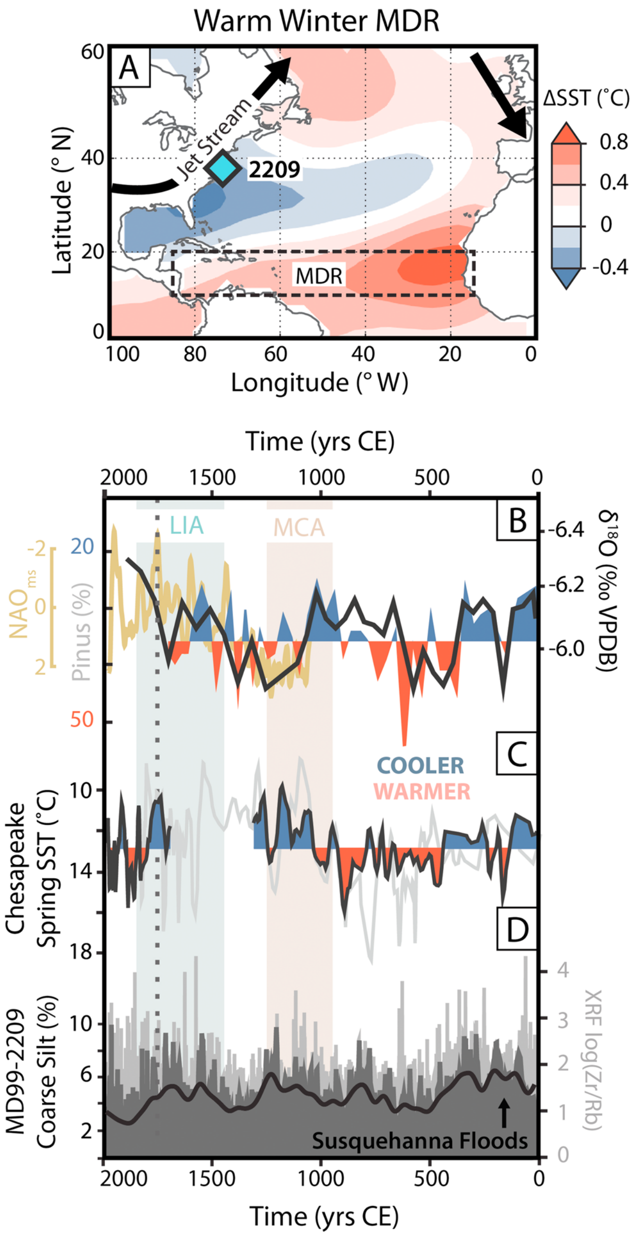

Figure 4. Comparison of MD99-2209 grain size to nearby North Atlantic Oscillation (NAO) and SST sensitive proxies. (a) Map of North Atlantic showing winter (JFM) ΔSST for years when Main Development Region (MDR) is anomalously warm compared to the long-term mean (adapted from X. Wang et al., 2017). (b) Dashed line indicates timing of post-European land clearance, based on ragweed pollen (Figure 2c). NAO reconstruction (Trouet et al., 2009; yellow)—axis reversed—overlain by calcite $\delta^{18}O$ record of Buckeye Creek Cave, West Virginia, speleothem (Hardt et al., 2010; black line) and pre-European settlement (only) pine percent data from MD99-2209 (Willard et al., 2003) shown by blue/red shading, interpreted as having cooler or warmer relative conditions. (c) Mg/Ca derived (5-pt Gaussian filtered) Spring SST reconstruction from MD99-2209 and RD98 (Cronin et al., 2003) shown in red/blue. Mg/Ca temperature data (gray line) from companion core MD03-2661 (Cronin et al., 2010) was graphically correlated to MD99-2209. (d) Percent coarse-silt from MD99-2009 (dark gray shaded). Black line shows 100-yr filtered percent coarse-silt data. Light gray shading shows XRF log (Zr/Rb) data. SST = sea surface temperature; LIA = Little Ice Age; MCA = Medieval Climate Anomaly.

500–200 CE (Bratton et al., 2003), indicating increased input of terrestrial organic carbon to Chesapeake Bay likely driven, in part, by increased Susquehanna River flooding. Its oxidation may have contributed to low bottom water oxygen conditions as indicated by high levels of leachable rhenium. Elevated levels of Re around 58.5 cm in RD98 (Baucom et al., 2001) likely followed fluvial deposition by Hurricane Agnes and serves as a modern analog for similar peaks found from ~1,800–1,400, 900–600, and 400–100 yr BP in MD99-2209 (Bratton et al., 2000). Postcolonial anoxia of Chesapeake Bay has largely been attributed to upstream land use change (e.g., Cooper & Brush, 1991), but large flood events on the Susquehanna River, like Tropical Storm Lee (2011), are thought to have contributed to further O_2 depletion (Testa & Kemp, 2014).

Our record is consistent with a potential link between flood frequency and winter temperatures in the Eastern United States through the NAO (Figure 4). Flood deposits in MD99-2209 correspond with intervals of lower pine pollen percentage in the same core, previously interpreted to reflect intrusion of polar air across Eastern North America (Willard et al., 2005; Figures 4b and 4d). Colder winter conditions in the mid-Atlantic could also explain intervals of lighter calcite $\delta^{18}O$ precipitation in a speleothem from nearby Buckeye Creek Cave, WV (Hardt et al., 2010). Increased cold event frequency over the continental United States is often indicative of negative phases of the NAO (Thompson & Wallace, 2001), and both records above bear similarities to the 1,000-year long NAO reconstruction of Trouet et al. (2009; Figure 4b). While the winter moisture budget (evaporation minus precipitation) over much of Eastern North America changes little between NAO phases (Hurrell, 1995), persistent weakness of the western end of the subtropical ridge—implied by more negative NAO conditions—is consistent with enhanced hurricane tracking toward the East Coast (e.g., Kossin et al., 2010). Increased hurricane rainfall may therefore explain, in part, intervals of increased flood frequency on the Susquehanna during the late Holocene as well as nearby rivers such as the Little Tennessee River, North Carolina-Tennessee (L. Wang & Leigh, 2012), and Greenbrier River, West Virginia (Aldred, 2010).

Negative NAO conditions may also foster stronger tropical cyclone genesis, overall, in the Main Development Region (~10–20° N, 20–85° W; Figure 4a). The negative phase of the NAO is often associated with colder than usual winter SSTs off the East Coast but anomalously warm conditions in the tropical North Atlantic. X. Wang et al. (2017) suggest that warm winter (January-March) SST anomalies in the tropical North Atlantic are related to increased tropical cyclone activity in the Main Development Region the following summer. We find more frequent deposition from large floods when Chesapeake Bay SSTs, based on Mg/Ca ostracodes measurements (Figure 4c), were colder than normal (Cronin et al., 2003, 2010). For example, of the grain-size peaks coarser than the inferred 1936 flood deposit (32–63-μm fraction), about two thirds occur when MD99-2209 Mg/Ca SST estimates (Figure 4c) were below their long-term mean. The large magnitude of these Chesapeake Bay temperature excursions relative to the more stable SST conditions that likely prevailed at low latitudes (e.g., Black et al., 2007) further supports the role of regional SST gradients in driving North Atlantic hurricane activity (Camargo et al., 2013).

5. Conclusions

We reconstructed major floods from the Susquehanna River during the last two millennia from sedimentary records collected in Northern Chesapeake Bay. Shallowly buried coarse-grained deposits, dated using ^{210}Pb, were laid-down during Hurricane Agnes (1972), the Great Flood of March 1936, and other large historic floods. Similar event layers that predate instrumented flow measurements occur downcore, with increased frequency between ~1800–1500, 1300–1100, and 400–0 CE. These intervals correspond with colder winter conditions near Chesapeake Bay that were likely caused by intrusions of Arctic air during negative phases of the NAO. Weakening of the western subtropical ridge, typical of negative NAO conditions, as well as warmer than usual, relative, SSTs in the Main Development Region could have led to increased hurricane related flooding on the Susquehanna and, possibly, along other Eastern rivers.

Acknowledgments
This work was supported by the USGS Land Change Science Program and Northeast Region. We appreciated the assistance of Brian Buczkowski, Andrew Zimmerman, and John Bratton in locating archived core materials and data sets. We thank John Jackson and Bryan Landacre for assistance with XRD and pollen analysis, respectively. We thank two anonymous reviewers, Lynn Wingard (USGS), and Rob Stamm (USGS) for their helpful feedback on earlier versions of this manuscript. Any use of trade, firm, or product names is for descriptive purposes only and does not imply endorsement by the U.S. Government. Data generated for this report can be found in the accompanying supporting information.

References

Aldred, J. L. (2010). The effects of late Holocene climate changes on flood frequencies and magnitudes in Central Appalachia, Ohio University.

Andersen, A. M., Davis, W. J., Lynch, M. P., & Schubel, J. (1973). Effects of Hurrican Agnes on the environment and organisms of Chesapeake Bay: Early findings and recommendations. V.I.M.S. Special Report in Marine Science and Ocean Egineering (29).

Appleby, P. G., & Oldfield, F. (1978). The calculation of lead-210 dates assuming a constant rate of supply of unsupported ^{210}Pb to the sediment. *Catena*, *5*(1), 1–8. https://doi.org/10.1016/S0341-8162(78)80002-2

Appleby, P. G., & Oldfield, F. (1983). The assessment of ^{210}Pb data from sites with varying sediment accumulation rates. *Hydrobiologia*, *103*(1), 29–35. https://doi.org/10.1007/BF00028424

Bailey, J. F., Patterson, J. L., & Paulhus, J. L. H. (1975). Hurricane Agnes rainfall and floods, June-July 1972. US Geological Survey Professional Paper 924 (371 p.). Retrieved from https://pubs.usgs.gov/pp/0924/report.pdf

Baucom, P. C., Bratton, J. F., Colman, S. M., Friddell, J., & Rochon, A. (2000). Sedimentology and core descriptions, Marion-Dufresne Cores MD99-2204 through -2209, Chesapeake Bay, Chapter 5. In T. M. Cronin (Ed.), *Initial report on IMAGES V cruise of the Marion-Defresne to the Chesapeake Bay, June 20–22, 199, USGS Open-File Report 00-306*. Retrieved from https://pubs.usgs.gov/of/2000/of00-306/chapter5/

Baucom, P. C., Bratton, J. F., Colman, S. M., Moore, J. M., King, J., Heil, C., & Seal, R. (2001). Selected data for sediment cores collected in Chesapeake Bay in 1996 and 1998, U.S. Geological Survey Open-File Report, 2001-194.

Black, D. E., Abahazi, M. A., Thunell, R. C., Kaplan, A., Tappa, E. J., & Peterson, L. C. (2007). An 8-century tropical Atlantic SST record from the Cariaco Basin: Baseline variability, twentieth-century warming, and Atlantic hurricane frequency. *Paleoceanography and Paleoclimatology*, *22*, PA4204. https://doi.org/10.1029/2007PA001427

Blanton, D. B., Chenoweth, M., & Mock, C. J. (2009). The Great Flood of 1771: An explanation of natural causes and social effects. In *Historical climate variability and impacts in North America*. Dordrecht; Heidelberg; London; New York: Springer.

Brandon, C. M., Woodruff, J. D., Lane, D., & Donnelly, J. P. (2013). Tropical cyclone wind speed constraints from resultant storm surge deposition: A 2500 year reconstruction of hurricane activity from St. Marks, FL. *Geochemistry, Geophysics, Geosystems*, *14*, 2993–3008. https://doi.org/10.1002/ggge.20217

Bratton, J. F., Colman, S. M., Baucom, P. C., & Seal, R. R. II (2000). Trace metals, stable isotopes, and biogenic silica from cores collected at Marion-Dufresne site MD99-2209, Chesapeake Bay, Chapter 10, In T. M. Cronin (Ed.), *Initial report on IMAGES V cruise of the Marion-Defresne to the Chesapeake Bay, June 20–22, 199, USGS Open-File Report 00–306*. Retrieved from https://pubs.usgs.gov/of/2000/of00-306/chapter10/

Bratton, J. F., Colman, S. M., & Seal, R. R. II (2003). Eutrophication and carbon sources in Chesapeake Bay over the last 2700 yr: Human impacts in context. *Geochimica et Cosmochimica Acta*, *67*(18), 3385–3402. https://doi.org/10.1016/S0016-7037(03)00131-5

Brush, G. S. (1984). Patterns of recent sediment accumulation in Chesapeake Bay (Virginia—Maryland, USA) tributaries. *Chemical Geology*, *44*(1–3), 227–242. https://doi.org/10.1016/0009-2541(84)90074-3

Camargo, S. J., Ting, M., & Kushnir, Y. (2013). Influence of local and remote SST on North Atlantic tropical cyclone potential intensity. *Climate Dynamics*, *40*(5–6), 1515–1529. https://doi.org/10.1007/s00382-012-1536-4

Cann, J., & Cronin, T. (2004). An association of benthic foraminifera and gypsum in Holocene sediments of estuarine Chesapeake Bay, USA. *The Holocene*, *14*(4), 614–620. https://doi.org/10.1191/0959683604hl738rr

Colman, S. M., Baucom, P. C., Bratton, J. F., Cronin, T. M., McGeehin, J. P., Willard, D., et al. (2002). Radiocarbon dating, chronologic framework, and changes in accumulation rates of Holocene estuarine sediments from Chesapeake Bay. *Quaternary Research*, *57*(01), 58–70. https://doi.org/10.1006/qres.2001.2285

Colman, S. M., Halka, J. P., & Iii, C. H. (1992). Patterns and rates of sediment accumulation in the Chesapeake Bay during the Holocene rise in sea level. In *Quaternary coasts of the United States: Marine and lacustrine systems*, *SEPM Special Publication* (Vol. 48, pp. 101–111). The Society for Sedimentary Geology (SEPM).

Cooper, S. R., & Brush, G. S. (1991). Long-term history of Chesapeake Bay anoxia. *Science*, *254*(5034), 992–996. https://doi.org/10.1126/science.254.5034.992

Cronin, T., Thunell, R., Dwyer, G., Saenger, C., Mann, M., Vann, C., & Seal, R. (2005). Multiproxy evidence of Holocene climate variability from estuarine sediments, eastern North America. *Paleoceanography and Paleoclimatology*, *20*, PA4006. https://doi.org/10.1029/2005PA001145

Cronin, T. M. (2004). Pocomoke sound sedimentary and ecosystem history. USGS Open-File Report 2004-1350 (141 p.). Retrieved from https://pubs.er.usgs.gov/publication/ofr20041350

Cronin, T. M., Dwyer, G. S., Kamiya, T., Schwede, S., & Willard, D. A. (2003). Medieval warm period, little ice age and 20th century temperature variability from Chesapeake Bay. *Global and Planetary Change*, *36*(1–2), 17–29. https://doi.org/10.1016/S0921-8181(02)00161-3

Cronin, T. M., Hayo, K., Thunell, R. C., Dwyer, G. S., Saenger, C., & Willard, D. (2010). The medieval climate anomaly and little ice age in Chesapeake Bay and the North Atlantic Ocean. *Palaeogeography, Palaeoclimatology, Palaeoecology*, *297*(2), 299–310. https://doi.org/10.1016/j.palaeo.2010.08.009

Cronin, T. M., Vogt, P., Willard, D., Thunell, R., Halka, J., Berke, M., & Pohlman, J. (2007). Rapid sea level rise and ice sheet response to 8,200-year climate event. *Geophysical Research Letters*, *34*, L20603. https://doi.org/10.1029/2007GL031318

Davies, S., Lamb, H., & Roberts, S. (2015). Micro-XRF Core Scanning in Palaeolimnology: Recent Developments. In I. Croudace & R. Rothwell (Eds.), *Micro-XRF Studies of Sediment Cores, Developments in Paleoenvironmental Research* (Vol. 17). Dordrecht, Netherlands: Springer.

Denommee, K., Bentley, S., & Droxler, A. (2014). Climatic controls on hurricane patterns: A 1200-y near-annual record from Lighthouse Reef, Belize. *Scientific Reports*, *4*, 3876.

Donnelly, J. P., & Woodruff, J. D. (2007). Intense hurricane activity over the past 5,000 years controlled by El Nino and the West African monsoon. *Nature*, *447*(7143), 465–468. https://doi.org/10.1038/nature05834

Eaton, A., Grant, V., & Gross, M. G. (1980). Chemical tracers for particle transport in the Chesapeake Bay. *Estuarine and Coastal Marine Science*, *10*(1), 75–83. https://doi.org/10.1016/S0302-3524(80)80050-8

Geyer, W. R. (1993). The importance of suppression of turbulence by stratification on the estuarine turbidity maximum. *Estuaries*, *16*(1), 113–125. https://doi.org/10.2307/1352769

Gross, M. G., Karweit, M., Cronin, W. B., & Schubel, J. (1978). Suspended sediment discharge of the Susquehanna River to northern Chesapeake Bay, 1966 to 1976. *Estuaries*, *1*(2), 106–110. https://doi.org/10.2307/1351599

Halka, J. P., Vogt, P. R., Colman, S. M., & Cronin, T. M. (2001). Geophysical environment: Site MD99-2209, Chapter 4. In T. M. Cronin (Ed.), *Initial report on IMAGES V cruise of the Marion-Defresne to the Chesapeake Bay, June 20–22, 199, USGS Open-File Report 00-306*. Retrieved from https://pubs.usgs.gov/of/2000/of00-306/chapter4/

Hardt, B., Rowe, H. D., Springer, G. S., Cheng, H., & Edwards, R. L. (2010). The seasonality of east central North American precipitation based on three coeval Holocene speleothems from southern West Virginia. *Earth and Planetary Science Letters*, *295*(3–4), 342–348. https://doi.org/10.1016/j.epsl.2010.04.002

Hart, R. E., & Evans, J. L. (2001). A climatology of the extratropical transition of Atlantic tropical cyclones. *Journal of Climate*, *14*(4), 546–564. https://doi.org/10.1175/1520-0442(2001)014<0546:ACOTET>2.0.CO;2

Hirschberg, D. J., & Schubel, J. (1979). Recent geochemical history of flood deposits in the northern Chesapeake Bay. *Estuarine and Coastal Marine Science*, *9*(6), 771–IN7. https://doi.org/10.1016/S0302-3524(79)80010-9

Hurrell, J. W. (1995). Decadal trends in the North Atlantic Oscillation: Regional temperatures and precipitation. *Science*, *269*(5224), 676–679. https://doi.org/10.1126/science.269.5224.676

Jones, P., Jonsson, T., & Wheeler, D. (1997). Extension to the North Atlantic Oscillation using early instrumental pressure observations from Gibraltar and south-west Iceland. *International Journal of Climatology: A Journal of the Royal Meteorological Society*, *17*(13), 1433–1450. https://doi.org/10.1002/(SICI)1097-0088(19971115)17:13<1433::AID-JOC203>3.0.CO;2-P

King, J. W., & Heil, C. W. (2000). Physical properties of Marion-Dufresne Cores MD-99 2204-2209 and magnetic secular variation studies of MD-99 2207, Chapter 11. In T. M. Cronin (Ed.), *Initial report on IMAGES V cruise of the Marion-Defresne to the Chesapeake Bay, June 20–22, 199, USGS Open-File Report 00-306*. Retrieved from https://pubs.usgs.gov/of/2000/of00-306/chapter11/

Kossin, J. P., Camargo, S. J., & Sitkowski, M. (2010). Climate modulation of North Atlantic hurricane tracks. *Journal of Climate*, *23*(11), 3057–3076. https://doi.org/10.1175/2010JCLI3497.1

Kunkel, K. E., Easterling, D. R., Kristovich, D. A., Gleason, B., Stoecker, L., & Smith, R. (2012). Meteorological causes of the secular variations in observed extreme precipitation events for the conterminous United States. *Journal of Hydrometeorology*, *13*(3), 1131–1141. https://doi.org/10.1175/JHM-D-11-0108.1

Milici, R. C., & Campbell, E. V. (1997). A predictive production rate life-cycle model for southwestern Virginia coalfields, USGS Circular 1147. Retrieved from https://pubs.usgs.gov/circ/c1147/

Moss, J. H., & Kochel, R. C. (1978). Unexpected geomorphic effects of the Hurricane Agnes storm and flood, Conestoga drainage basin, southeastern Pennsylvania. *The Journal of Geology*, *86*(1), 1–11. https://doi.org/10.1086/649652

Munoz, S. E., Giosan, L., Therrell, M. D., Remo, J. W., Shen, Z., Sullivan, R. M., et al. (2018). Climatic control of Mississippi River flood hazard amplified by river engineering. *Nature*, *556*(7699), 95–98. https://doi.org/10.1038/nature26145

NCDC. (2018). NOAA National Centers for Environmental information, Climate at a Glance: Statewide Time Series.

Nie, Y., Suayah, I. B., Benninger, L. K., & Alperin, M. J. (2001). Modeling detailed sedimentary ^{210}Pb and fallout ^{239,240}Pu profiles to allow episodic events: An application in Chesapeake Bay. *Limnology and Oceanography*, *46*(6), 1425–1437. https://doi.org/10.4319/lo.2001.46.6.1425

Officer, C. B., Lynch, D. R., Setlock, G. H., & Helz, G. R. (1984). Recent sedimentation rates in Chesapeake Bay. In V. S. Kennedy (Ed.), *The estuary as a filter* (pp. 131–157). New York: Elsevier. https://doi.org/10.1016/B978-0-12-405070-9.50013-X

Oliva, F., Viau, A. E., Bjornson, J., Desrochers, N., & Bonneau, M.-A. (2016). A 1300 year reconstruction of paleofloods using oxbow lake sediments in temperate southwestern Quebec, Canada. *Canadian Journal of Earth Sciences*, *53*(4), 378–386. https://doi.org/10.1139/cjes-2015-0191

Orth, R. J., & Moore, K. A. (1984). Distribution and abundance of submerged aquatic vegetation in Chesapeake Bay: An historical perspective. *Estuaries*, *7*(4), 531–540. https://doi.org/10.2307/1352058

Palinkas, C. M., Halka, J. P., Li, M., Sanford, L. P., & Cheng, P. (2014). Sediment deposition from tropical storms in the upper Chesapeake Bay: Field observations and model simulations. *Continental Shelf Research*, *86*, 6–16. https://doi.org/10.1016/j.csr.2013.09.012

Powers, M. C. (1954). Clay diagenesis in the Chesapeake Bay area. In *Clays and clay minerals: NatlResearch Council Pub* (Vol. 327, pp. 68–80). New York: Pergamon, Oxford.

Ramsey, C. B. (2008). Deposition models for chronological records. *Quaternary Science Reviews*, *27*(1–2), 42–60. https://doi.org/10.1016/j.quascirev.2007.01.019

Reimer, P. J., Bard, E., Bayliss, A., Beck, J. W., Blackwell, P. G., Ramsey, C. B., et al. (2013). IntCal13 and Marine13 radiocarbon age calibration curves 0–50,000 years cal BP. *Radiocarbon*, *55*(04), 1869–1887. https://doi.org/10.2458/azu_js_rc.55.16947

Ryan, J. D. (1953). The sediments of Chesapeake Bay, Johns Hopkins University.

Schubel, J., & Pritchard, D. (1986). Responses of upper Chesapeake Bay to variations in discharge of the Susquehanna River. *Estuaries*, *9*(4), 236–249. https://doi.org/10.2307/1352096

Schubel, J. R. (1974). Effects of tropical storm Agnes on the suspended solids of the northern Chesapeake Bay. In R. J. Gibbs (Ed.), *Suspended solids in water* (pp. 113–132). Boston, MA: Springer.

Sturdevant-Rees, P., Smith, J. A., Morrison, J., & Baeck, M. L. (2001). Tropical storms and the flood hydrology of the central Appalachians. *Water Resources Research*, *37*(8), 2143–2168. https://doi.org/10.1029/2000WR900310

Testa, J. M., & Kemp, W. M. (2014). Spatial and temporal patterns of winter–spring oxygen depletion in Chesapeake Bay bottom water. *Estuaries and Coasts*, *37*(6), 1432–1448. https://doi.org/10.1007/s12237-014-9775-8

Thompson, D. W., & Wallace, J. M. (2001). Regional climate impacts of the Northern Hemisphere annular mode. *Science*, *293*(5527), 85–89. https://doi.org/10.1126/science.1058958

Toomey, M. R., Korty, R. L., Donnelly, J. P., van Hengstum, P. J., & Curry, W. B. (2017). Increased hurricane frequency near Florida during Younger Dryas Atlantic Meridional Overturning Circulation slowdown. *Geology*, *45*(11), 1047–1050. https://doi.org/10.1130/G39270.1

Trouet, V., Esper, J., Graham, N. E., Baker, A., Scourse, J. D., & Frank, D. C. (2009). Persistent positive North Atlantic Oscillation mode dominated the medieval climate anomaly. *Science*, *324*(5923), 78–80. https://doi.org/10.1126/science.1166349

USGS (2018). National Water Information System data. Retrieved from http://waterdata.usgs.gov/nwis/

Villarini, G., Goska, R., Smith, J. A., & Vecchi, G. A. (2014). North Atlantic tropical cyclones and US flooding. *Bulletin of the American Meteorological Society*, *95*(9), 1381–1388. https://doi.org/10.1175/BAMS-D-13-00060.1

Walter, R. C., & Merritts, D. J. (2008). Natural streams and the legacy of water-powered mills. *Science*, *319*(5861), 299–304. https://doi.org/10.1126/science.1151716

Wang, L., & Leigh, D. S. (2012). Late-Holocene paleofloods in the Upper Little Tennessee River valley, Southern Blue Ridge Mountains, USA. *The Holocene*, *22*(9), 1061–1066. https://doi.org/10.1177/0959683612437863

Wang, X., Liu, H., & Foltz, G. R. (2017). Persistent influence of tropical North Atlantic wintertime sea surface temperature on the subsequent Atlantic hurricane season. *Geophysical Research Letters*, *44*, 7927–7935. https://doi.org/10.1002/2017GL074801

Willard, D. A., Bernhardt, C. E., Korejwo, D. A., & Meyers, S. R. (2005). Impact of millennial-scale Holocene climate variability on eastern North American terrestrial ecosystems: Pollen-based climatic reconstruction. *Global and Planetary Change*, *47*(1), 17–35. https://doi.org/10.1016/j.gloplacha.2004.11.017

Willard, D. A., Cronin, T. M., & Verardo, S. (2003). Late-Holocene climate and ecosystem history from Chesapeake Bay sediment cores, USA. *The Holocene*, *13*(2), 201–214. https://doi.org/10.1191/0959683603hl607rp

Zabawa, C., & Schubel, J. (1974). Geologic effects of tropical storm Agnes on upper Chesapeake Bay. *Maritime Sediments*, *10*(3), 79–84.